MKPH-T-96-6

The position and the residues of the delta resonance pole in pion photoproduction

O. Hanstein, D. Drechsel and L. Tiator

Institut für Kernphysik, Universität Mainz, 55099 Mainz, Germany

Abstract

We have analyzed the $M_{1+}^{(3/2)}$ and $E_{1+}^{(3/2)}$ multipole amplitudes of pion photoproduction in the framework of fixed-t dispersion relations. Applying the speed plot technique to our results for these multipoles, we have determined the position and the residues of the Δ (1232) resonance pole. The pole is found at total *c.m.* energy $W = (1211 - 50i)$ MeV on the second Riemann sheet, and the ratio of the electric and magnetic residues is $R_\Delta = -0.035 - 0.046i$, resulting in an E2/M1 ratio for the "dressed" delta resonance of -3.5%.

PACS numbers: 13.60.Le, 14.20.Gk, 11.55.Fv, 11.80.Et

Keywords: Pion photoproduction, electromagnetic properties of the delta resonance, speed plot, dispersion relations

I. INTRODUCTION

The determination of the quadrupole excitation strength $E_{1+}^{(3/2)}$ in the region of the $\Delta(1232)$ resonance has been the aim of considerable experimental and theoretical activities. Within the harmonic oscillator quark model, the Δ and the nucleon are both members of the symmetrical 56-plet of $SU(6)$ with orbital momentum $L = 0$, positive parity and a Gaussian wave function in space. In this approximation the Δ may only be excited by a magnetic dipole transition $M_{1+}^{(3/2)}$ [1]. However, in analogy with the atomic hyperfine interaction or the forces between nucleons, also the interactions between the quarks contain a tensor component due to the exchange of gluons. This hyperfine interaction admixes higher states to the nucleon and Δ wave functions, in particular d-state components with $L = 2$, resulting in a small electric quadrupole transition $E_{1+}^{(3/2)}$ between nucleon and Δ [2–4], and a quadrupole moment of the Δ $Q_\Delta \approx -.09 fm^2$ [5]. Therefore an accurate measurement of $E_{1+}^{(3/2)}$ is of great importance in testing the forces between the quarks and, quite generally, models of nucleons and isobars.

The ratio

$$R_{EM} = \frac{\mathrm{Re}\left[E_{1+}^{(3/2)} M_{1+}^{(3/2)*}\right]}{\mid M_{1+}^{(3/2)} \mid^2} \tag{1}$$

has been predicted to be in the range $-2\% \leq R_{EM} < 0\%$ in the framework of constituent quark [2,4,5], relativized quark [6–8] and chiral bag models [9,10]. Considerably larger values have been obtained in Skyrme models [11]. A first lattice QCD calculation resulted in a small value with large error bars ($-6\% \leq R_{EM} \leq 12\%$) [12]. However, the connection of the model calculations with the experimental data is not evident. Clearly, the Δ resonance is coupled to the pion-nucleon continuum and final-state interactions will lead to strong background terms seen in the experimental data, particularly in case of the small E_{1+} amplitude. The question of how to "correct" the experimental data to extract the properties of the resonance has been the topic of many theoretical investigations. As some typical examples we refer the reader to the work of Olsson [13], Koch et al. [14] and Laget [15]. Unfortunately

it turns out that the analysis of the small E_{1+} amplitude is quite sensitive to details of the models, e.g. nonrelativistic vs. relativistic resonance denominators, constant or energy-dependent widths and masses of the resonance, sizes of the form factor included in the width etc. In other words, by changing these definitions the meaning of resonance vs. background changes, too. More recently, Nozawa et al. [16] have included final-state interactions in a dynamical model with quark cores and pions, and Davidson et al. [17] have analyzed photoproduction in terms of effective Lagrangians, taking account of final-state interactions implicitly through unitarization. By fitting the parameters of the models to older sets of data, Ref. [16] obtained a ratio $R_{EM}^{\mathrm{bare}\ \Delta} = -3.1\%$ for the bare $\gamma N\Delta$ coupling, while Ref. [17] deduced a value of $R_{EM}^{\mathrm{res}} = -1.4\%$, including some "dressing" from final-state interaction. A detailed discussion of these models and a comparison to the data is given in Ref. [18]. In an extension of the work of Nozawa et al., Bernstein et al. [19] have decomposed the multipole contributions into resonant and background terms, and compared their analysis to previous investigations. As a result they obtained $R_{EM}^{\mathrm{bare}\ \Delta} = -(3.1 \pm 1.3)\%$ for the "bare Δ" amplitude and $R_{EM}^{\mathrm{res}} = -2.2\%$ for the "dressed Δ". In very recent relativistic and unitarized pion photoproduction calculations, for the "bare Δ" ratios of $R_{EM}^{\mathrm{bare}\ \Delta} = -1.43\%$ [20] and $R_{EM}^{\mathrm{bare}\ \Delta} = -1.46\%$ [21] are found.

In order to study the Δ deformation, pion photoproduction on the proton has recently been measured by the LEGS collaboration [22] at Brookhaven and by the A2 collaboration [23] at MAMI using transversely polarized photons, i.e. by measuring the polarized photon asymmetry Σ. In particular, the cross section $d\sigma_{\parallel}$ for photon polarization in the reaction plane turns out to be very sensitive to the small E_{1+} amplitude. Assuming for simplicity that only the P-wave multipoles contribute, the differential cross section is

$$\frac{d\sigma_{\parallel}}{d\Omega} = \frac{q}{k}(A_{\parallel} + B_{\parallel}\cos\Theta_{\pi} + C_{\parallel}\cos^2\Theta_{\pi}), \tag{2}$$

where q and k are the pion and photon momenta and Θ_{π} is the pion emission angle in the *c.m.* frame. Neglecting the (small) contributions of the Roper multipole M_{1-}, one obtains [23]

$$C_\parallel/A_\parallel \approx 12 R_{EM}, \tag{3}$$

because the isospin $\frac{3}{2}$ amplitudes strongly dominate the cross section for π^0 production. In the meantime new precision data have been obtained by the A2 collaboration at MAMI with polarized photons for both charged and neutral pion production over the energy range 270 MeV $\leq E_\gamma \leq$ 420 MeV [23,24]. These data will make it possible to determine the partial wave amplitudes over the full region of the Δ resonance. The preliminary data for π^0 production are in good agreement with the ratio $d\sigma_\parallel/d\sigma_\perp$ measured by the LEGS collaboration, at the lower energies.

II. DISPERSION RELATIONS AT FIXED t

Starting from fixed-t dispersion relations for the invariant amplitudes of pion photoproduction, the projection of the multipole amplitudes leads to a well known system of integral equations,

$$\mathrm{Re}\mathcal{M}_l(W) = \mathcal{M}_l^{\mathrm{P}}(W) + \frac{1}{\pi}\sum_{l'} \mathcal{P}\int_{W_{\mathrm{thr}}}^{\infty} K_{ll'}(W,W')\mathrm{Im}\mathcal{M}_{l'}(W')dW', \tag{4}$$

where $\mathcal{M}_l$ stands for any of the multipoles $E_{l\pm}$, $M_{l\pm}$, and $\mathcal{M}_l^{\mathrm{P}}$ for the corresponding (nucleon) pole term. The kernels $K_{ll'}$ are known, and the real and imaginary parts of the amplitudes are related by unitarity. In the energy region below two-pion threshold, unitarity is expressed by the final state theorem of Watson [25],

$$\mathcal{M}_{\updownarrow}^{\mathcal{I}}(\mathcal{W}) = \mid \mathcal{M}_{\updownarrow}^{\mathcal{I}}(\mathcal{W}) \mid \rceil^{\rangle(\delta_{\updownarrow}^{\mathcal{I}}(\mathcal{W})+\backslash\pi)}, \tag{5}$$

where δ_l^I is the corresponding πN phase shift and n an integer. We have essentially followed the method of Schwela et al [26,27] to solve Eqs. (4) with the constraint (5). In addition we have taken account of the coupling to some higher states neglected in that earlier reference. At the energies above two-pion threshold up to $W = 2$ GeV, Eq. (5) has been replaced by an ansatz based on unitarity [26]. Finally, the contribution of the dispersive integrals from 2 GeV to infinity has been replaced by t-channel exchange, parametrized by certain fractions

of ρ- and ω-exchange. Furthermore, we have to allow for the addition of solutions of the homogeneous equations to the coupled system of Eq. (4). The whole procedure introduces 9 free parameters, which have to be determined by a fit to the data. In our data base we have included the recent MAMI experiments for π° and π^+ production off the proton in the energy range from 160 MeV to 420 MeV [28,24,29], both older and more recent data from Bonn for π^+ production off the proton [30–32], and older Frascati [33] and more recent TRIUMF data [34] on π^- production off the neutron. As shown in Fig. 1, the predicted cross sections are in perfect agreement with the ratio $d\sigma_\parallel/d\sigma_\perp$ measured by the LEGS collaboration [22,35] whose data have not been included in our fit. In Fig. 2 we show our result for the ratio R_{EM} which is in general agreement with the analysis of the Virginia group [36].

III. THE RESONANCE POLE PARAMETERS AS DETERMINED BY THE SPEED PLOT

The analytic continuation of a resonant partial wave as function of energy into the second Riemann sheet should generally lead to a pole in the lower half-plane. A pronounced narrow peak reflects a time-delay in the scattering process due to the existence of an unstable excited state. This time-delay is related to the speed SP of the scattering amplitude T, defined by [37,38]

$$SP(W) = \left| \frac{dT(W)}{dW} \right|, \tag{6}$$

where W is the total $c.m.$ energy. In the vicinity of the resonance pole, the energy dependence of the full amplitude $T = T_B + T_R$ is determined by the resonance contribution,

$$T_R(W) = \frac{r\Gamma_R e^{i\phi}}{M_R - W - i\Gamma_R/2} \ , \tag{7}$$

while the background contribution T_B should be a smooth function of energy, ideally a constant. We note in particular that $W_R = M_R - i\Gamma_R/2$ indicates the position of the resonance pole in the complex plane, i.e. M_R and Γ_R are constants and differ from the

energy-dependent widths, and possibly masses, derived from fitting certain resonance shapes to the data [39]. If the energy dependence of T_B is negligible, the speed is

$$SP(W) = r\Gamma_R \frac{\{[(M_R - W)^2 - \Gamma_R^2/4]^2 + \Gamma_R^2 (M_R - W)^2\}^{\frac{1}{2}}}{\{(M_R - W)^2 + \Gamma_R^2/4\}^2}. \tag{8}$$

Obviously the speed has its maximum at $W = M_R$, $SP(M_R) = 4r/\Gamma_R = H$, and the half-maximum values are $SP(M_R \pm \Gamma_R/2) = H/2$. This determines the parameters M_R and Γ_R as well as the absolute value r of the residue. The phase ϕ of the complex residue at the pole may be determined from an Argand plot of the speed vector dT/dW.

It should be noted that the speed plot technique requires a reasonably smooth representation of the amplitude in order to differentiate it in a meaningful way. As has been shown by Höhler [37,38] in the case of πN scattering, dispersion relations are particularly well suited for this purpose. If we apply the method to the partial waves obtained by solving Eqs. (4), the results for the Δ multipole clearly show a resonant peak, but the asymmetry with respect to the maximum indicates an energy dependence of the background (see Fig. 3). This effect may be traced back to the nucleon pole terms. After subtracting these well-defined terms from the amplitudes, the speed of both E_{1+} and M_{1+} can be well described according to Eq. (7). Fig. 4 shows a comparison of this procedure to the ideal shape of a resonance pole and the resulting Argand diagrams for the speed vector. Except for the threshold region, the differences are almost invisible. Having determined all the resonance parameters, we can now decompose the full amplitudes into contributions of the resonance pole and background terms. As may be seen in Fig. 5, the background is a relatively smooth function of energy without any structure around the resonance. However, the background is quite large, in particular in the case of the E_{1+} amplitude.

The resonance parameters derived from our analysis are shown in Table I. It is seen that the pole position $W_R = M_R - i\Gamma_R/2 = (1211 - 50i)$ MeV is in excellent agreement with the results obtained from πN scattering, $M_R = (1210 \pm 1)$ MeV and $\Gamma_R = 100$ MeV [37–39] . This agreement may not be very surprising in the case of the largely resonant M_{1+} amplitude, for which there exist earlier investigations to determine the pole position

[40,41]. However, it is much less obvious that the interference pattern of Re E_{1+} of Fig. 5 should lead to the same answer. The excellent agreement in that case, too, is indeed very satisfactory and shows that the speed plot technique is quite reliable for the extraction of resonance properties. The table also shows the absolute values and the phases of the resonance residues. Because of the different backgrounds in the two amplitudes, ϕ_M and ϕ_E are different, and the ratio of the resonance amplitudes is complex. The fact that the two "apple shaped" structures in Fig. 4 are essentially oriented in opposite direction is, however, related to the negative value of R_{EM} for the full (experimental) amplitude. Concerning the resonance pole contributions alone, we obtain

$$R_\Delta = \frac{r_E e^{i\phi^E}}{r_M e^{i\phi_M}} = -0.035 - 0.046i. \tag{9}$$

The ratio of the heights of the speed plots is $H_E/H_M = r_E/r_M = 5.8\%$. We hasten to add, however, that the experimental observable is related to the real part of the ratio (see Eq. 1), i.e. the (unphysical) case of the resonance without background would lead to $R_{EM}^{\rm res}$ =Re$(R_\Delta) = -3.5\%$.

As has been mentioned before, the ratio for the full (experimental) amplitudes is real below two-pion threshold due to the Watson theorem. As may be seen from Fig. 2, this ratio $R_{EM}(W)$ is strongly dependent on energy, and increases with energy from negative to positive values, e.g. $R_{EM}(M_R - \Gamma_R/2) = -10.4\%$, $R_{EM}(M_R) = -4.3\%$, $R_{EM}(M_R + \Gamma_R/2) = 0.1\%$. The resonance pole in the complex plane, $M_R - i\Gamma_R/2$, and the nonresonant background lead to a πN phase shift $\delta_{1+} = 90^\circ$ at $W = M_\Delta = 1232$ MeV. Due to the Watson theorem, both $E_{1+}^{(3/2)}$ and $M_{1+}^{(3/2)}$ are completely imaginary at this point, and the ratio can be determined from the experimental data as $R_{EM}(M_\Delta)$ =Im$E_{1+}^{(3/2)}(M_\Delta)$/Im$M_{1+}^{(3/2)}(M_\Delta)$. The recent, nearly model-independent value of the Mainz group at $W = M_\Delta$ is $(-2.5 \pm 0.2)\%$ [23,24].

IV. CONCLUSION

It has been shown that the method of speed plots can be well applied to analyze the pion photoproduction amplitudes. The resonance pole position of the $\Delta(1232)$ is obtained from these amplitudes in excellent agreement with the results from pion-nucleon scattering. The complex residues of the resonance pole terms give information on those parts of the full amplitude that have a resonance–like behaviour. Whether such a contribution originates from a "bare" resonance or, e.g. from a nonresonant pion production followed by rescattering into a resonant state, is model-dependent [42] and cannot be answered by an analysis of the data but only within the framework of a specific model.

In the future it will be interesting to analyze double polarization variables, e.g. both photon and recoil or target polarization, because some of these observables turn out to be very sensitive to electric quadrupole radiation, too. It is also worthwhile pointing out that reactions like $e\vec{p} \to e'p\pi^\circ$ yield a longitudinal-transverse interference term ("fifth structure function"), which is sensitive to the imaginary part of the interference between the resonant and background multipoles.

ACKNOWLEDGMENTS

We would like to thank Prof. G. Höhler for very fruitful discussions and the members of the A2 collaboration at Mainz for providing us with their preliminary data, in particular R. Beck, F. Härter and H.-P. Krahn. This work was supported by the Deutsche Forschungsgemeinschaft (SFB 201).

REFERENCES

[1] C. M. Becchi and G. Morpurgo, Phys. Lett. 17 (1965) 352.

[2] R. Koniuk and N. Isgur, Phys. Rev. D 21 (1980) 1868.

[3] S. S. Gershteyn and G. V. Dzhikiya, Sov. J. Nucl. Phys. 34 (1981) 870.

[4] N. Isgur, G. Karl and R. Koniuk, Phys. Rev. D 25 (1982) 2394.

[5] D. Drechsel and M. M. Giannini, Phys. Lett. 143 B (1984) 329.

[6] J. Bienkowska, Z. Dziembowski and H. J. Weber, Phys. Rev. Lett. 59 (1987) 624.

[7] S. Capstick and G. Karl, Phys. Rev. D 41 (1990) 2767.

[8] S. Capstick, Phys. Rev. D 46 (1992) 2864.

[9] G. Kälbermann and J. J. Eisenberg, Phys. Rev. D 28 (1983) 71 and D 29 (1984) 517.

[10] K. Bermuth, D. Drechsel, L. Tiator and J. B. Seaborn, Phys. Rev. D 37 (1988) 89.

[11] A. Wirzba and W. Weise, Phys. Lett. B 188 (1987) 6.

[12] D. B. Leinweber, T. Draper and R. Woloshyn, Contribution to Baryons '92, p. 29 (1992).

[13] M. G. Olsson, Nucl. Phys. B 78 (1974) 55.

[14] J. H. Koch, E. J. Moniz and N. Ohtsuka, Ann. Phys. (N. Y.) 154 (1984) 99.

[15] J. M. Laget, Nucl. Phys. A 481 (1988) 765.

[16] S. Nozawa, B. Blankleider and T.–S. Lee, Nucl. Phys. A 513 (1990) 513.

[17] R. M. Davidson, N. C. Mukhopadhyay and R. Wittman, Phys. Rev. Lett. 56 (1986) 804 and Phys. Rev. D 43 (1991) 71.

[18] M. A. Khandaker et al., πN Newsletter 8 (1993) 114.

[19] A. M. Bernstein, S. Nozawa and M. A. Moinester, Phys. Rev. C 47 (1993) 1274.

[20] M. Vanderhaeghen, K. Heyde, J. Ryckebusch, and M. Waroquier, preprint SSF95-05-01, Gent (1995).

[21] Y. Surya and F. Gross, preprint CEBAF-TH-95-04 (1995).

[22] G. S. Blanpied et al., Phys. Rev. Lett. 69 (1992) 1880.

[23] R. Beck, Proc. Int. Conf. "Baryons '95", Santa Fé, (1995).

[24] H.–P. Krahn, Ph.D. thesis, Mainz (1996).

[25] K. M. Watson, Phys. Rev. 95 (1954) 228.

[26] D. Schwela and R. Weizel, Z. Physik 221 (1969) 71.

[27] W. Pfeil and D. Schwela, Nucl. Phys. B 45 (1972) 379.

[28] M. Fuchs et al., Phys. Lett. B 368 (1996) 20.

[29] F. Härter, PhD. thesis, Mainz (1996).

[30] D. Menze, W. Pfeil and R. Wilcke, Compilation of pion photoproduction data, Bonn (1977).

[31] K. Buechler et al., Nucl. Phys. A 570 (1994) 580.

[32] H. Dutz, PhD. thesis, Bonn (1993),
D. Krämer, PhD. thesis, Bonn (1993),
B. Zucht, PhD. thesis, Bonn (1995).

[33] F. Carbonara et al., Nuovo Cim. 13 A (1973) 59.

[34] A. Bagheri et al., Phys. Rev. C 38 (1988) 875.

[35] A. Sandorfi, private communication (1996), release L7a8.0.

[36] R. A. Arndt, I. I. Strakovsky and R. L. Workman, Phys. Rev. C 53 (1996) 430.

[37] G. Höhler and A. Schulte, πN Newsletter 7 (1992) 94.

[38] G. Höhler, πN Newsletter 9 (1993) 1.

[39] Review of Particle Properties, Phys. Rev. D 50 (1994).

[40] R. R. Campbell, G. L. Shaw and J. S. Ball, Phys. Rev. D 14 (1976) 2431.

[41] I. I. Miroshnichenko, V. I. Nikiforov, V. M. Sanin, P. V. Sorokin, and S. V. Shalatskii, Sov. J. Nucl. Phys. 29 (1979) 94.

[42] P. Wilhelm, Th. Wilbois and H. Arenhövel, preprint MKPH-T-96-1, Mainz (1996).

TABLES

TABLE I. Resonance pole parameters determined by applying of the speed plot technique to our results for $E_{1+}^{(\frac{3}{2})}$ and $M_{1+}^{(\frac{3}{2})}$.

	r [10^{-3}MeV/m$_\pi$]	ϕ [°]	M_R [MeV]	Γ_R [MeV]
E	1.23	-154.7	1211±1	102±2
M	21.16	-27.5	1212±1	99±2

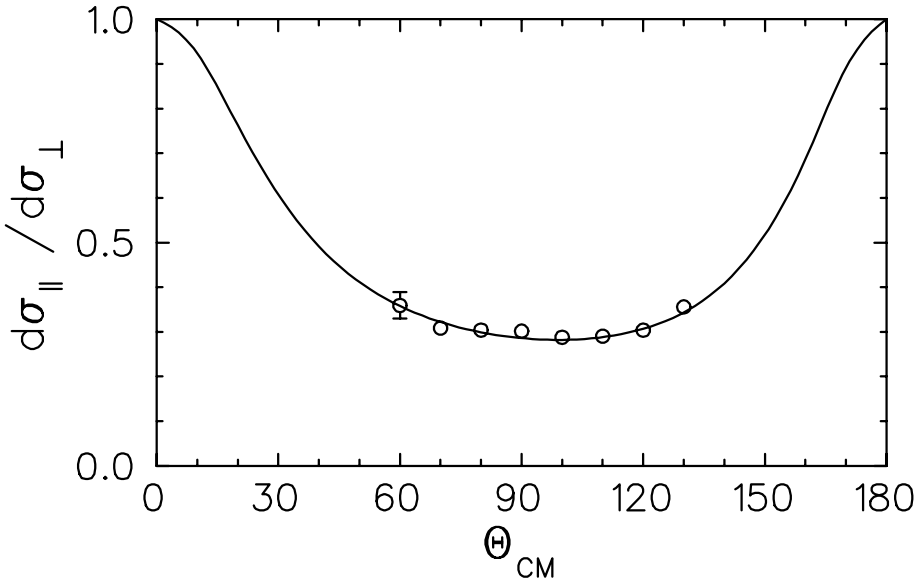

FIG. 1. Ratio $d\sigma_{\parallel}/d\sigma_{\perp}$ of the differential cross section for $\mathrm{p}(\gamma,\pi^0)\mathrm{p}$ at photon *lab.* energy $E_\gamma = 333$ MeV. The solid line is our result from dispersion analysis. The data are from [35].

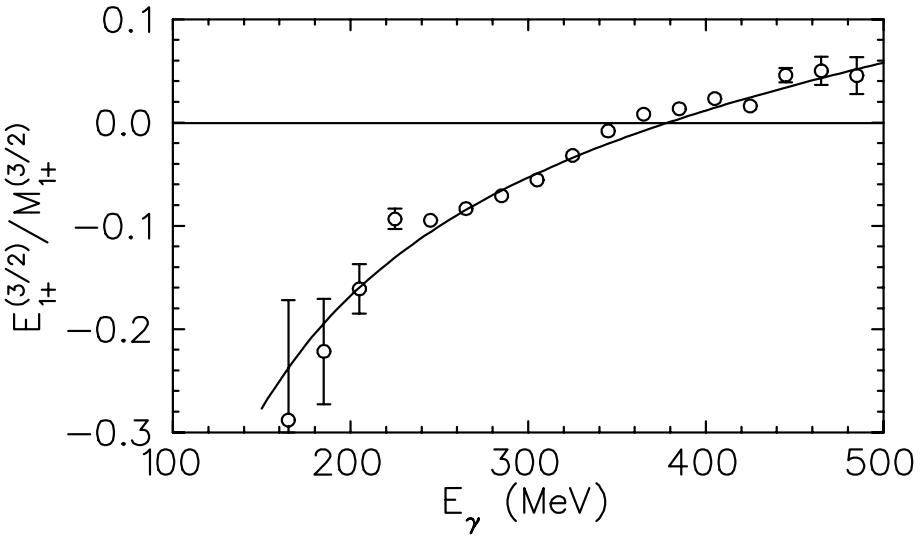

FIG. 2. Ratio of the electric and magnetic 3,3-multipoles as a function of the photon *lab.* energy. The solid line is the result of our dispersion analysis, the data points are from the VPI analysis [36].

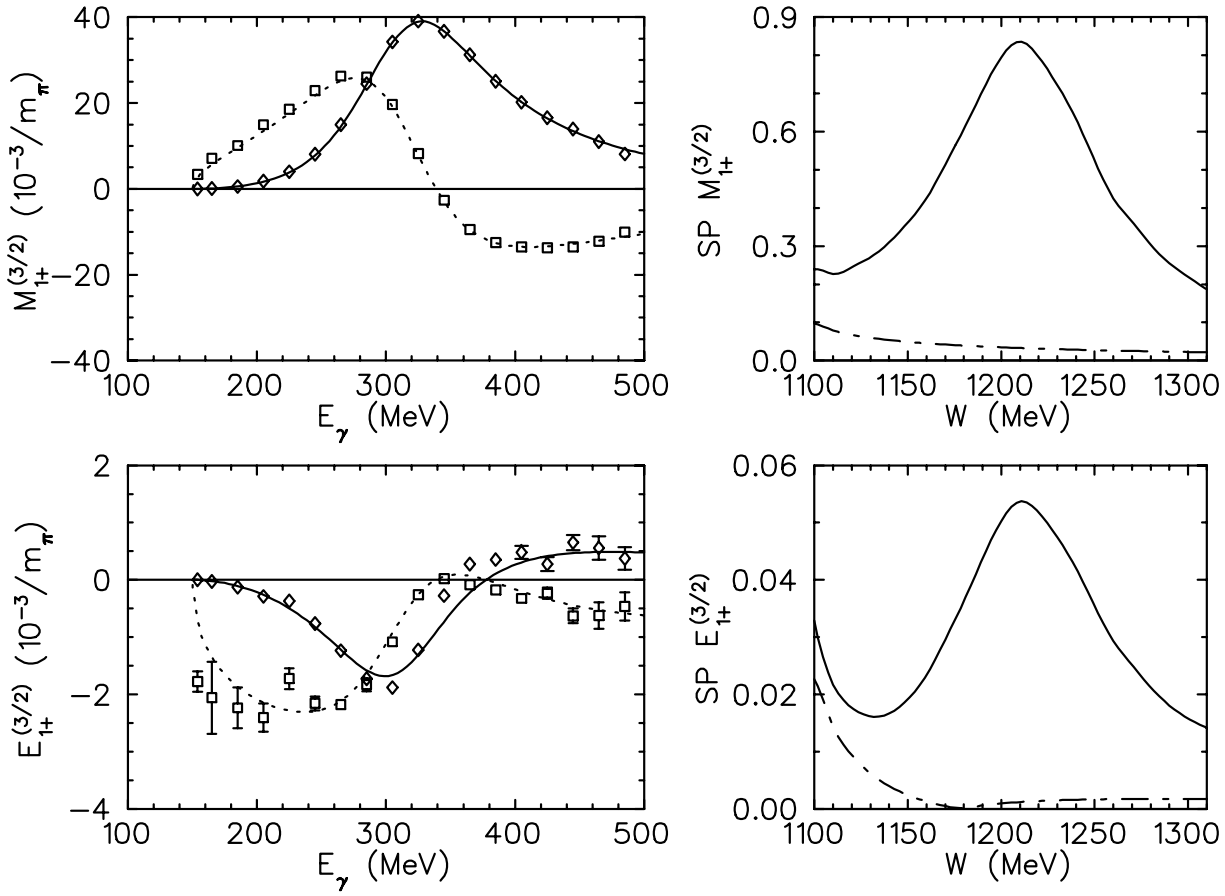

FIG. 3. Our results for real (dotted lines) and imaginary (solid lines) parts of $M_{1+}^{(\frac{3}{2})}$ and $E_{1+}^{(\frac{3}{2})}$ together with the speed plots of the full amplitudes. The dashed-dotted lines are the derivatives of the (nucleon) pole term contributions. The data are from the VPI analysis [36].

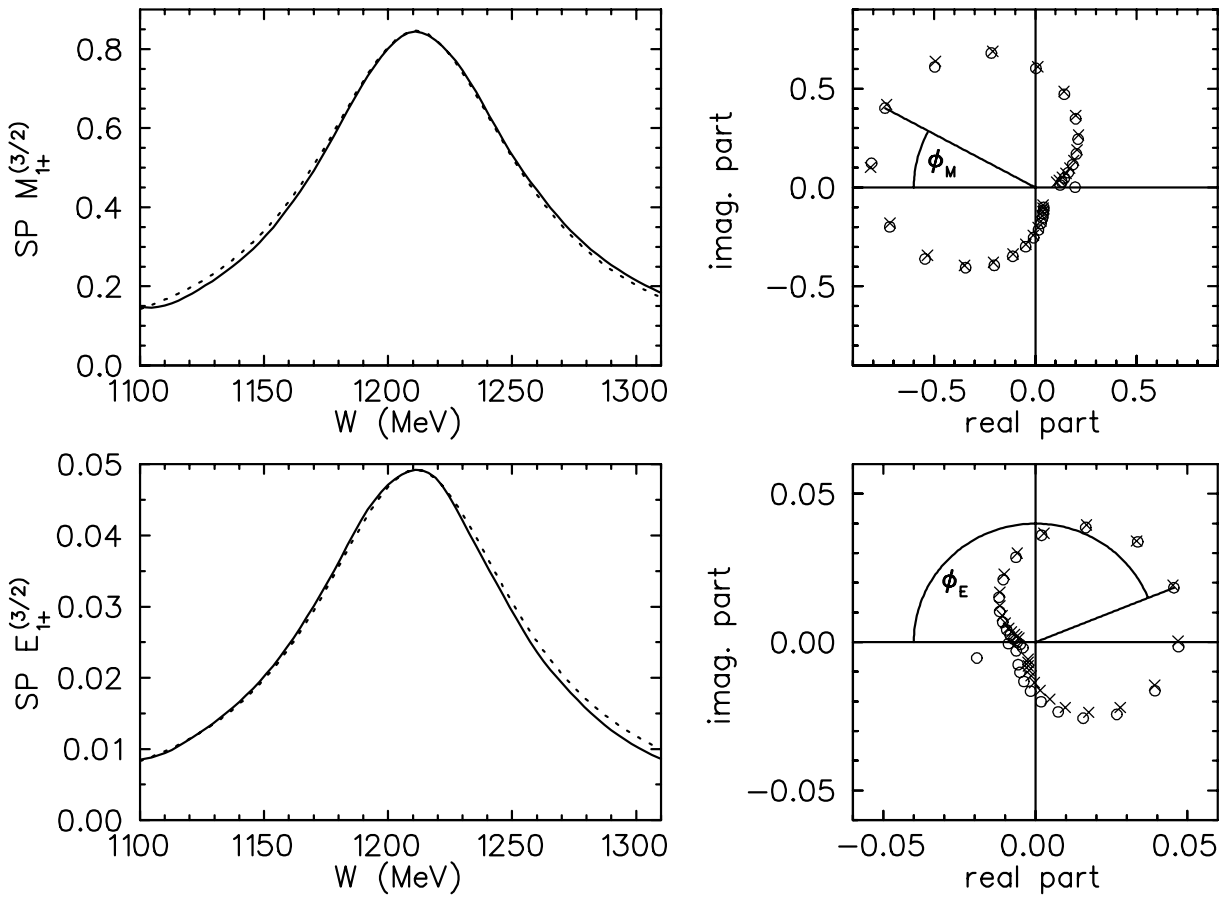

FIG. 4. Speed of $M_{1+}^{(\frac{3}{2})}$ and $E_{1+}^{(\frac{3}{2})}$ after subtraction of the (nucleon) pole term contributions (solid lines). For comparison we show the speed of an ideal resonance pole with the parameters given in Table I (dotted lines). In the Argand diagrams of the speed vectors we also compare our result (circles) with the speed corresponding to an exact pole (crosses). The only discrepancies are due to threshold effects.

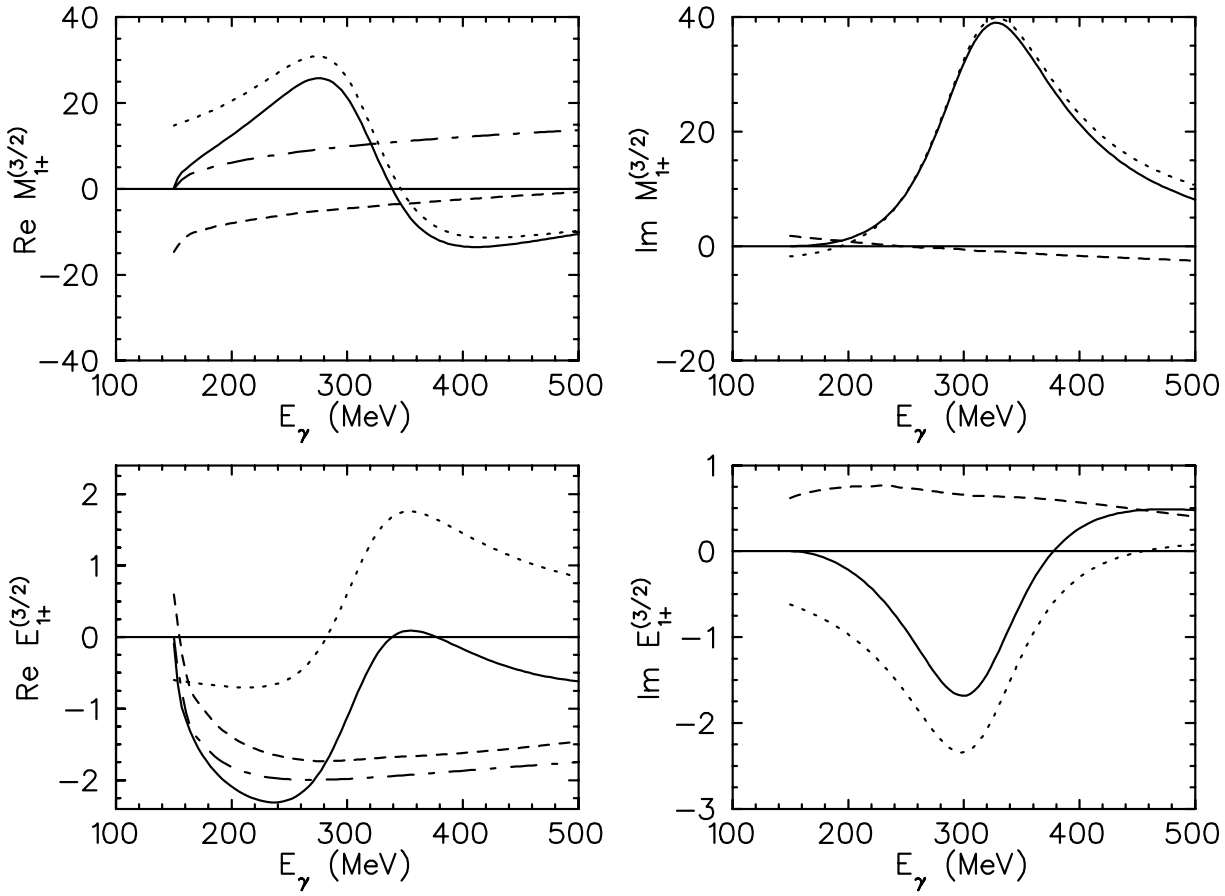

FIG. 5. Separation of resonance and background contributions for the 3,3-multipoles. Solid lines: full amplitude, dotted lines: contribution of resonance pole, dashed lines: background, dash-dotted lines: (nucleon) pole term contribution.